energies

MDPI

Article

Facile Synthesis of Lanthanum Strontium Cobalt Ferrite (LSCF) Nanopowders Employing an Ion-Exchange Promoted Sol-Gel Process

Sri Rahayu [1,2], Adi Ab Fatah [1] and Girish M. Kale [1,*]

[1] School of Chemical and Process Engineering, University of Leeds, Leeds LS2 9JT, UK; pmsr@leeds.ac.uk (S.R.); adihaniftatah@gmail.com (A.A.F.)
[2] Center for Materials Technology, Agency for Assessment and Application of Technology, Puspiptek Building 224 Tangerang Selatan, Serpong, South Tangerang 15314, Indonesia
* Correspondence: g.m.kale@leeds.ac.uk; Tel.: +44-(0)113-343-2805

Abstract: The perovskite nanopowders of lanthanum strontium cobalt ferrite (LSCF) have been synthesized using the alginate mediated ion-exchange process. This perovskite-based material is a promising cathode for intermediate-temperature solid oxide fuel cells (IT-SOFCs) due to its high electrical conductivity, low polarizability, high catalytic activity for oxygen reduction, enhanced chemical stability at an elevated temperature in high oxygen potential environment and high compatibility with the ceria based solid electrolytes. Phase pure LSCF 6428, LSCF 6455, and LSCF 6482 corresponding to $La_{0.6}Sr_{0.4}Co_{0.2}Fe_{0.8}O_{3-\delta}$, $La_{0.6}Sr_{0.4}Co_{0.5}Fe_{0.5}O_{3-\delta}$, and $La_{0.6}Sr_{0.4}Co_{0.8}Fe_{0.2}O_{3-\delta}$, respectively were successfully synthesized. The simultaneous thermal analysis (DSC-TGA) and XRD were used to determine the optimum calcination temperature for the dried ion-exchanged beads. Single phase nanopowders of LSCF (6428, 6455, and 6482) have been successfully prepared at a calcination temperature of 700 °C. The TGA analysis showed that every ton of LSCF-ALG dried beads can potentially yield 360 kg of LSCF nanopowders suggesting a potential for scaling-up of the process of manufacturing nanopowders of LSCF.

Keywords: LSCF; nanopowders; perovskite; intermediate temperature-solid oxide fuel cells (IT-SOFCs); cathode material

Citation: Rahayu, S.; Fatah, A.A.; Kale, G.M. Facile Synthesis of Lanthanum Strontium Cobalt Ferrite (LSCF) Nanopowders Employing an Ion-Exchange Promoted Sol-Gel Process. *Energies* **2021**, *14*, 1800. https://doi.org/10.3390/en14071800

Academic Editors: Vladislav A. Sadykov and Bahman Amini Horri

Received: 8 February 2021
Accepted: 22 March 2021
Published: 24 March 2021

1. Introduction

The modern solid oxide fuel cells (SOFCs) are akin to other fuel cell designs as they are capable of generating electricity directly from the reaction between hydrogen gas, natural gas or syngas at the anode with the oxide ions produced at the cathode and transported across the solid electrolyte membrane to the anode. The cells have the highest operating temperature of all the fuel cell types which is around 800 to 1000 °C. They benefit from the high operating temperature as reaction kinetics are enhanced leading to the elimination of the requirement for the catalyst and yielding high power efficiency. Due to their eco-friendly and efficient operation, SOFCs are utilized extensively in large and small stationary power generation [1].

Regardless of current advances in the technology, there are still substantial problems to commercializing SOFCs as an energy source to the wider population. Their high operating temperature restricts the choice of appropriate materials, decreases the endurance of the cells, costs more to build the cells, lowers the long-lasting stability, and takes a longer time for the start-up and shutdown [2]. Reducing the operating temperature to 500–800 °C can overcome most of the drawbacks and consequently has introduced this as the new objective in the SOFC research and development. The challenge nowadays is to develop materials with superior performance for intermediate temperature solid oxide fuel cells (IT-SOFCs). Oxygen reduction is known to be responsible for the considerable loss in

performance efficiency of SOFC, thus the catalytic activity of the cathode material and its internal structure has been researched and improved through several methods in recent times. One of the methods is through using mixed ionic-electronic conducting cathodes such as nanostructured perovskite-based materials having a larger surface area yielding a greater triple-phase boundary area to help increase the performance of IT-SOFCs [3]. Therefore, recent attention is focused on the development of new cathode materials having a perovskite structure with high catalytic efficiency for oxygen reduction and solid electrolyte materials having high oxide-ion conductivity and transference number close to unity.

Lanthanum strontium cobalt ferrite (LSCF) is a ceramic material exhibiting mixed ionic-electronic conducting properties with reasonably high electronic conductivity (200 s/cm) and good ionic conductivity (0.2 s/cm) [4]. Furthermore, LSCF has exceptional chemical and thermal stabilities at an elevated temperature and at high oxygen potentials as well as high catalytic activity for the oxygen reduction. However, the main issue of the LSCF material is Sr segregation at the surface of the electrode material [5]. Simner et al. also observed the segregation of Sr on both the outer and inner surfaces of the LSCF electrode after operation at 750 °C for 500 h [5,6]. The synthesis method, particle size of powders, powder composition, homogeneity and calcination or sintering temperature is known to have a considerable effect on the final morphology and microstructure of LSCF cathode used for the electrochemical cell. To obtain a pure LSCF material, various processing methods have been employed such as solid-state ceramic, co-precipitation, auto-combustion, sol-gel method, and more recently carbohydrate ion-exchange, but from a commercial standpoint, it is vital to be able to synthesize large quantities of LSCF nanopowders rapidly in an environmentally friendly and profitable way [7].

Therefore, the main objective of this research is to employ a novel cation-exchange process recently developed by Sardar et al. [8] called the Leeds alginate process (LAP) for three different compositions of LSCF nanopowders from sodium alginate as an organic ion-exchange medium for cations in a mixed homogeneous solution containing appropriate amounts of lanthanum, strontium, cobalt, and iron cations. The most interesting aspect of this study is that this is the first time LAP is applied to synthesize complex functional ceramic oxide nanopowders consisting of four different cations in three different stoichiometric ratios. Alginate, also known as alginic acid, is an anionic polysaccharide that occurs naturally in a large quantity, from 30 to 60% on a dry weight basis, in the cell walls of brown algae. It contains numerous amounts of 1,4′-linked β-D-mannuronic acid (M) and α-L-guluronic acid (G) residues in which the carboxylic acid functional group promotes gelation to form spherical beads when it interacts with multivalent metal ions. The obtained LSCF nanopowders after calcination of dried ion-exchanged beads are characterized using differential scanning calorimetry and thermogravimetric analysis (DSC-TGA), X-ray diffraction (XRD), and transmission electron microscopy (TEM). Further details of nanopowder preparation are given in the following section.

2. Materials and Methods

High purity >99% of lanthanum nitrate (La $(NO_3)_3$ $6H_2O$), and >95% of strontium nitrate (Sr $(NO_3)_2$), cobalt nitrate (Co $(NO_3)_2$ $6H_2O$), iron nitrate (Fe $(NO_3)_3$ $9H_2O$), as well as sodium alginate (Na-ALG) were procured from Fischer Scientific Ltd., UK. The chemical formula of LSCF with the stoichiometric elemental composition labelled as 6428, 6455, and 6482 are $La_{0.6}Sr_{0.4}Co_{0.2}Fe_{0.8}O_{3-\delta}$, $La_{0.6}Sr_{0.4}Co_{0.5}Fe_{0.5}O_{3-\delta}$, and $La_{0.6}Sr_{0.4}Co_{0.8}Fe_{0.2}O_{3-\delta}$, respectively. The nanopowders were prepared by the alginate mediated ion-exchange process known as LAP reported earlier by Kale et al. [7–9]. The precursor salts and organic precursor of sodium alginate were stirred separately in a beaker with the help of a magnetic stirrer. The organic alginate gel was dripped into a homogeneous salt solution, containing the required stoichiometric amounts of metal ions, using a syringe to form wet beads which were maintained in contact with the salt solution with gentle stirring to promote the ion-exchange reaction for a significant length of time. The wet beads were sieved and placed in a convection oven until they were completely dried. The diameter of beads

shrunk by nearly 50% on drying is shown in Figure 1. The dried beads were calcined at 500, 600, and 700 °C for 2 h in ambient atmosphere, to transform the metal ion-beads into multicomponent oxide nanopowders.

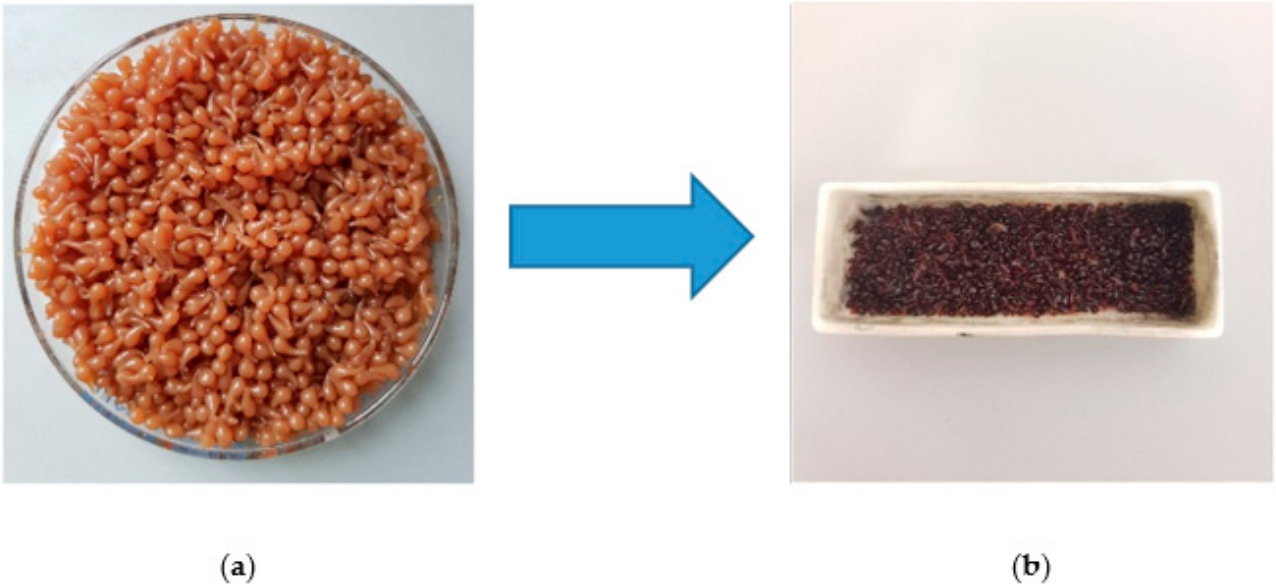

(a) (b)

Figure 1. (**a**) Lanthanum strontium cobalt ferrite-alginate (LSCF-ALG) wet beads and (**b**) dried beads.

The thermal analysis was performed using simultaneous DSC-TGA in flowing air at the rate of 10 cc min^{-1} and at the heating rate of 10 °C min^{-1} using the Mettler Toledo Star System to observe the signatures of phase transformation. The X-ray diffraction analysis (XRD) of nanopowders was performed using a P'Analytical X'Pert MPD with scans ranging from 20 to 80°. The TEM were carried out on the FEI Titan Themis 300 conducted on the calcined nanopowders.

3. Results

3.1. Thermal Analysis

Figure 2 shows the simultaneous thermal analysis results in which DSC and TGA traces were recorded at the same time. The thermal analysis was done to investigate the decomposition process of three different compositions of dried beads from which the calcination temperature could be determined. A common trend in the flowing air atmosphere was noticeable in all the TGA profiles for each of the compositions of LSCF indicating a four-step precursor bead decomposition and the product formation process. These steps could be described as follows:

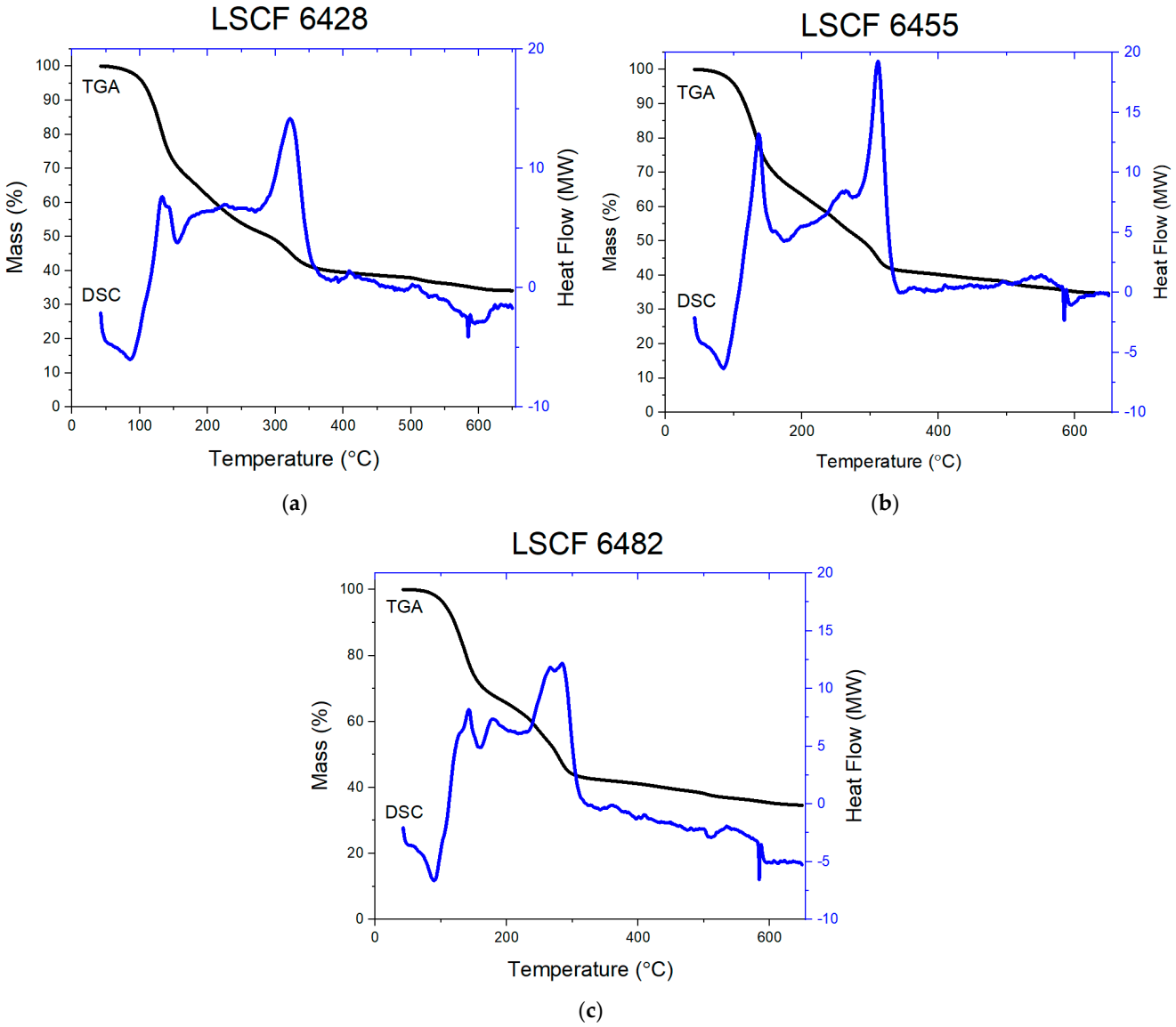

Figure 2. Thermal analysis of: (**a**) LSCF 6428; (**b**) LSCF 6455; (**c**) LSCF 6482.

1. At low temperature around 100 °C, the initial dehydration of beads occurred liberating any bound water molecules. The samples first absorbed heat from the surroundings to have enough kinetic energy to release bound water molecules. This caused endothermic peaks in the DSC profile matching to a small weight loss in the TGA profile.
2. At higher temperature (100–300 °C), the decomposition peak was exothermic due to the on-going oxidative decomposition of the dried beads. A large loss in weight was observed in the TGA profile due to the breakage of G-G, G-M, and M-M weaker linkages in the alginate polysaccharide molecule causing a substantial liberation of bridging oxygen. At once, this stimulated the oxidation of La^{3+}, Sr^{2+}, Co^{2+}, and Fe^{3+} in the alginate structure to form a mixture of the respective metastable metal oxides phases.
3. The further decomposition occurred as the temperature increased (300–500 °C) and resulted in a small weight loss in the TGA profile, which was caused by the decomposition of metastable oxides to more stable oxides (La_2O_3, SrO, CoO, and Fe_2O_3) that manifested in a small exothermic peak.

4. The further increase in temperature, around 500 °C, entirely oxidized the remaining β-D-manuronic acid (M) and α-L-guluronic acid (G), as well as the simultaneous formation of LSCF pseudoquaternary compound leading to the large exothermic peak in the DSC profile.

Any further increase in the temperature up to 700 °C did not show a significant measurable deviation in the TGA trace for all the three compositions indicating that a thermodynamically stable crystalline phase composition state has been reached.

3.2. Material Characterization

The XRD result for LSCF 6428 calcined at different temperatures of 500, 600, and 700 °C for a typical duration of 2 h are presented in Figure 3a. Using the X'pert HighScore software, the XRD pattern can be matched with the International Centre for Diffraction Data (ICDD) reference data for LSCF (00-064-0218). The major diffraction peaks in the synthesized compound agrees reasonably well with the reference pattern with some minor additional peaks observed at a lower calcination temperature, which are identified by closed red circles in Figure 3a.

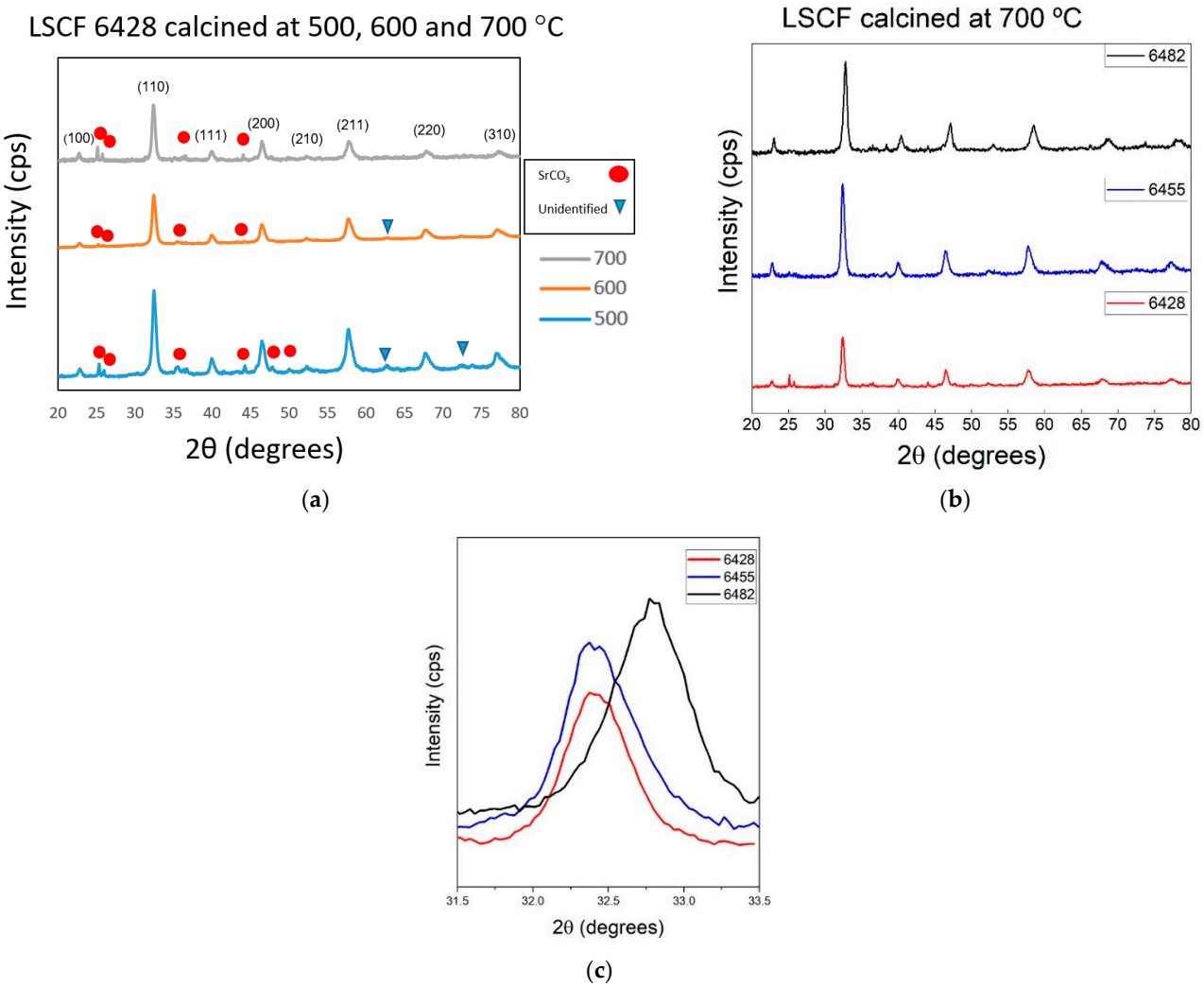

Figure 3. (**a**) XRD of calcined powders of LSCF 6428 at 500, 600, and 700 °C for 2 h; (**b**) comparison of XRD pattern of different compositions of LSCF calcined at 700 °C for 2 h; (**c**) comparison of (110) peak position of LSCF 6428, 6455, and 6482 calcined at 700 °C for 2 h.

The calcination temperature of 700 °C was used to further investigate LSCF with the additional two compositions, particularly LSCF 6455 and LSCF 6482. By changing the local environment around the B-site of the perovskite structure brought about by altering the ratio of Co/Fe in LSCF, the resulting XRD pattern shown in Figure 3b is seen to undergo a slight shift to the right for both LSCF 6455 and LSCF 6482. The shift can be seen clearly around the main peak when zooming in, as shown in Figure 3c.

The particle morphology and selected electron area diffraction (SAED) patterns of the nanopowders of LSCF of three different compositions are shown in Figure 4a–c. The square and hexagonal mixed morphologies of the nanoparticles of LSCF seen in Figure 4a–c confirm that the crystal structure of perovskite LSCF is mainly orthorhombic. Furthermore, the SAED pattern provides ample evidence that the nanoparticles are fully crystalline.

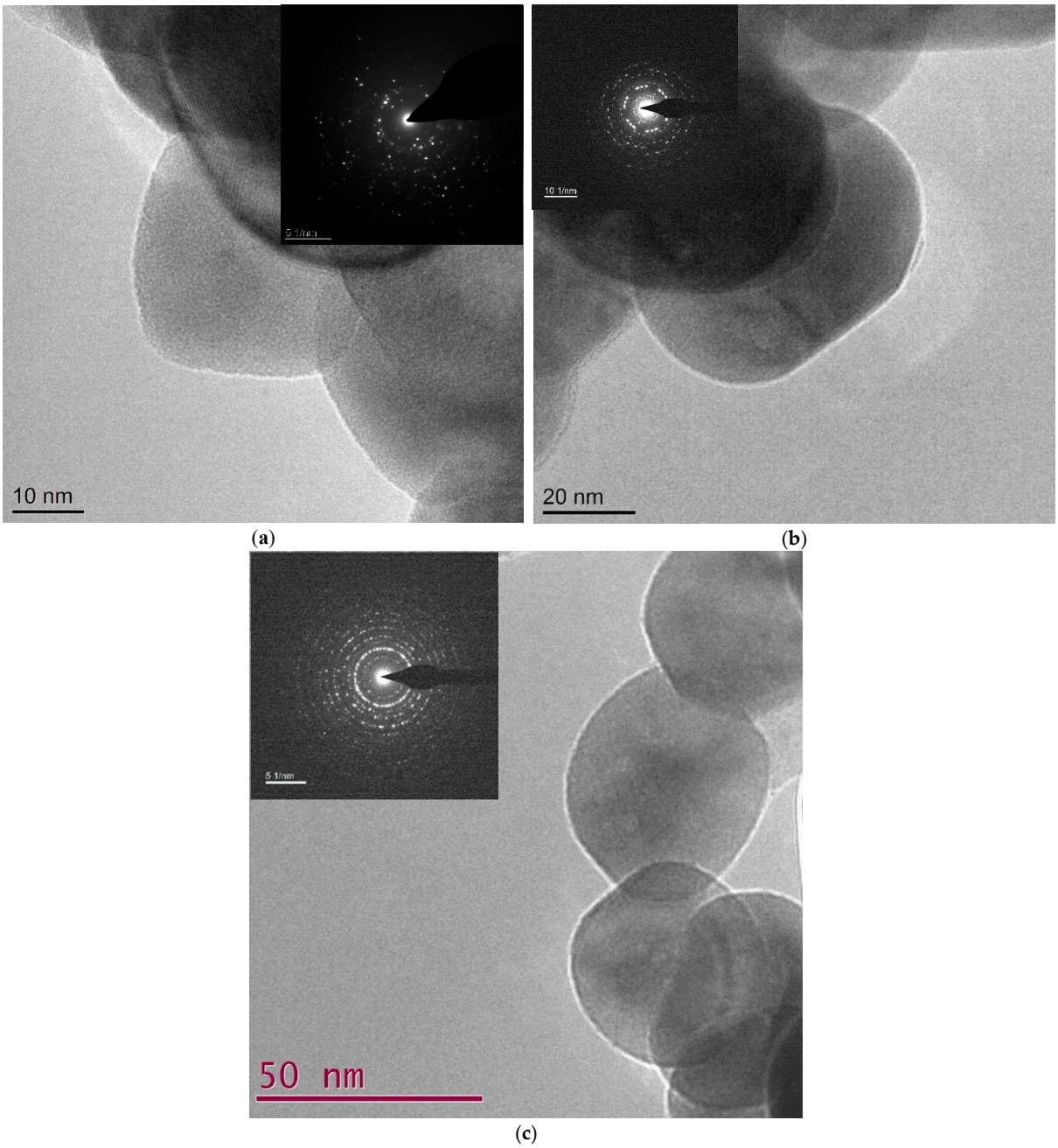

Figure 4. TEM images and selected electron area diffraction (SAED) patterns of calcined LSCF 6428 (**a**), 6455 (**b**), and 6482 (**c**) at 700 °C for 2 h.

The values of interplanar spacing (d-spacing) calculated from the morphology of the particles and selected electron area diffraction (SAED) patterns were compared with XRD in Table 1.

Table 1. Comparison of LSCF d-spacing values obtained by TEM with XRD data.

LSCF	Miller Indices	XRD	TEM
	h k l	(Å)	(Å)
6428	1 0 0	3.907	3.933
	1 1 0	2.767	2.937
	1 1 1	2.257	2.377
	2 0 0	1.953	1.991
6455	1 0 0	3.901	3.872
	1 1 0	2.769	2.826
	1 1 1	2.253	2.362
	2 0 0	1.958	1.954
6482	1 0 0	3.865	3.865
	1 1 0	2.729	2.826
	1 1 1	2.232	2.259
	2 0 0	1.926	1.996

Figure 5 shows the d-spacing at (100) peak calculated from XRD data against the ratio of Co/(Co + Fe) content in LSCF. It is clearly shown that increasing the Co content on the B-site can lead to decreasing the d-spacing in the compound.

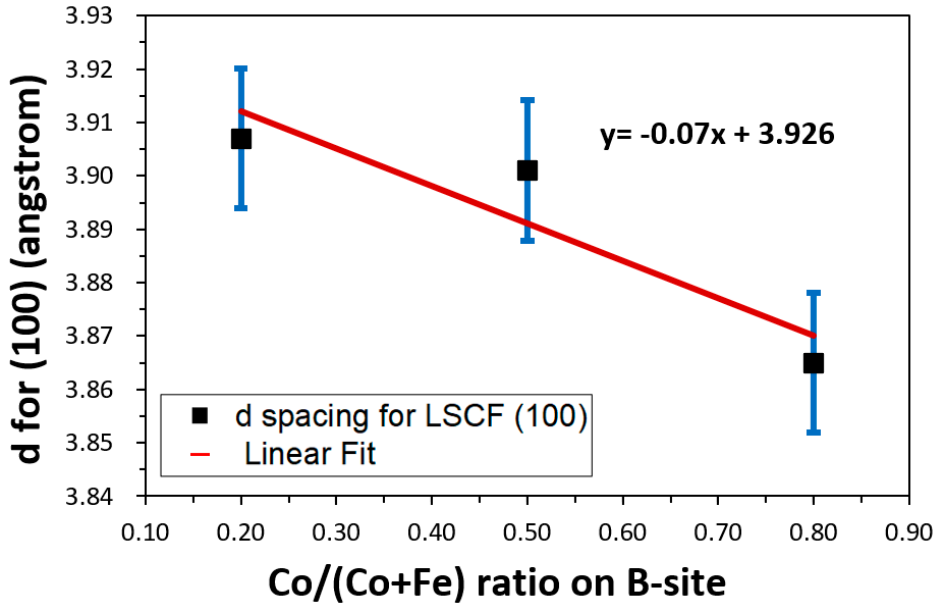

Figure 5. The d-spacing against the ratio of Co/(Co + Fe) in the LSCF.

4. Discussion

The thermal analysis was carried out to investigate the decomposition process of three different compositions of dried cation exchanged alginate beads for the determination of the calcination temperature of each of the LSCF composition. A common trend in the flowing air atmosphere was noticeable in all the TGA profiles for all the three compositions of LSCF which indicated a four-step decomposition process.

It can be seen in Figure 2a–c that a very small percentage of weight loss occurred according to the TGA profile beyond 600 °C suggesting that the composition of LSCF had reached a stable value. Therefore, a calcination temperature of approximately 15% higher,

i.e., 700 °C was chosen for the bulk product calcination to ensure a complete formation of LSCF from the dried ion exchanged beads. It was found that 11 mg of LSCF-ALG dried beads yielded 4 mg of LSCF nanopowders suggesting a 64% weight loss throughout the process. Therefore, as a conservative estimate, it can be expected that the alginate process can yield 360 kg of LSCF nanopowders per ton of dried LSCF-ALG beads.

However, this four-step process needs to be further scrutinized since there was a minor additional peak noticed in the DSC profile around 200–300 °C for both LSCF 6455 and 6482. It shows an additional endothermic decomposition step in this temperature range. This is believed to be due to the anhydrous strontium nitrate that was used as a precursor compound for the preparation of the aqueous ionic solution for the cation exchange process. According to Kosanke et al. [10], despite the anhydrous nature of strontium nitrate, there was a possibility of the presence of surface adsorbed water molecules in it. This was validated by the hygroscopic tendency of the material and consequently possesses a tendency to absorb water from the surrounding humid air which could clarify the endothermic drop after the exothermic peak between 200–300 °C. Furthermore, Wang et al. [7,11] stated that alginate in some measures offered some of its heat of combustion to the calcination process, hence, the alginate mediated ion-exchange process possibly generated net heat in the process and made this process more energy efficient. This has been shown independently by Sardar et al. in their recent work for the synthesis of $Ho_2Zr_2O_7$ [1] and $Ho_2Hf_2O_7$ [12] by an identical process.

Figure 3a exhibits the XRD pattern of perovskite phase with the minor secondary phase corresponding to the residual $SrCO_3$ [2] in 6428 but not in 6455 and 6482, i.e., with the increasing Co/Co + Fe ratio. Conceição et al. [2] also detected the presence of secondary phases in the LSCF material due to the incomplete combustion from the processes. The secondary phase formation was expected due to the reaction between the CO_2 present in the atmospheric air and the metal oxide formed during the calcination processes as seen in the previous investigation of the thermodynamic stability of ternary oxides in the Ba-Y-O system by Kale and Jacob [13]. The absence of $SrCO_3$ in 6455 and 6482 is probably due to the excess thermodynamic stability of LSCF crystal structure offered by the presence of higher Co content in LSCF compositions. Furthermore, in most synthetic processes used in the literature for preparing complex materials such as LSCF involving alkaline earth metals, the common reason usually attributed behind the emerging of secondary phase in XRD pattern is due to one or more phases formation as a result of the unwanted reaction, incomplete decomposition or phase segregation [14] at lower temperatures.

Furthermore, with the increase in the calcination temperature from 500 to 700 °C, the number of secondary phase and unidentified peaks decreased from eight peaks to four peaks at 700 °C. As expected, the calcination temperature was found to affect the phase purity of LSCF compositions synthesized by the alginate method. This result is akin to the finding of Cheng et al. [15] in which one of the compositions synthesized in this study namely the LSCF 6428 was calcined to four different calcination temperatures to obtain the phase pure compound of interest. Similarly, Kuhn and Ozkan [16] also studied the same material with different calcination temperatures by monitoring the change of perovskite phase leading to a final product, which was the single phase LSCF 6428. Both these studies [15,16] confirm that the single phase LSCF 6428 can be obtained by increasing the calcination temperature of LSCF precursor mix, which is in support of the current investigation of the three different compositions of LSCF, however, at the expense of an increase in the crystallite/particle size.

A lattice contraction trend was observed with the increasing Co content on the B-site. The interplanar spacing (d-value) shifted into a smaller value (Figure 5) and changed the peak position to a higher diffraction angle (Figure 3b). The deviation of d-spacing of (100) plane is at maximum for the 6428 composition, whereas 6455 and 6428 become progressively less. This could be due to the presence of excess $SrCO_3$ in 6428, whereas there is no sign of $SrCO_3$ seen in the other two compositions in XRD. The peak shift to the higher diffraction angle from (110) peak is shown in Figure 3c. Moreover, Table 1 also shows the

evidence of lattice contraction in d-spacing from XRD and TEM. This contraction occurred since the Co cation (CN 6, Co^{3+} = 61 pm) substituted Fe (CN 6, Fe^{3+} = 64.5 pm) ions that have a higher ionic radius [17].

TEM images in Figure 4a–c show that the average particle size of the LSCF nanopowders synthesized using the alginate method were 32, 42, and 53 nm for LSCF 6428, 6455, and 6482, respectively. The trend shows that as the cobalt content increases, the particle size increases. The larger particle size or thickness is also corroborated by the lack of visible lattice planes in the crystals in the TEM image and also by the presence of the spotted SAED pattern rather than the diffused rings around the central spot. The particle growth is most probably due to the grain growth that occurred during the calcination stage at 700 °C.

5. Conclusions

Perovskite LSCF nanopowders of varying Co/Fe ratios have been successfully synthesized using the alginate mediated ion-exchange process through the sol-gel technique at low temperatures. The thermal analysis of DSC-TGA was conducted on the dried beads under flowing air atmosphere, which was followed by XRD characterization of calcined dried beads to determine the optimum calcination temperature, which was found to be 700 °C for 2 h. Appropriate due diligence must be exercised in the preparation of LSCF compositions in particular at lower concentrations of Co/Co + Fe ratios to avoid formation of unwanted traces of $SrCO_3$. The process could potentially yield approximately 360 kg of LSCF nanopowders or the required composition from a ton of the dried beads. The appearance of unidentified peaks due to secondary impurity phases in the XRD pattern for samples calcined at lower temperatures could be easily eliminated at 700 °C. The Co/Fe ratio had a significant effect on the particle size of the LSCF albeit in a nanometer scale. The d-spacing values obtained from ICDD, the morphology of the nanoparticles, and SAED pattern of the nanoparticles were comparable for all the three compositions of LSCF synthesized in this study.

Author Contributions: The research strategy and experimental procedure as well as advise for characterization was conceptualized by G.M.K.; the research work was jointly supervised by the postgraduate researcher, S.R., in G.M.K.'s research group; the MSc research project student, A.A.F., was trained in the laboratory for conducting experiments by S.R.; the data analysis and writing of the article was done by all the authors involved in this article namely G.M.K., S.R. and A.A.F. All authors have read and agreed to the published version of the manuscript.

Funding: This research received no external funding.

Institutional Review Board Statement: Not applicable.

Informed Consent Statement: Not applicable.

Data Availability Statement: The raw data can be found on the instrument linked storage device at the University of Leeds and it can be made available on request to anyone interested in the future by contacting G.M.K. directly.

Acknowledgments: S.R. gratefully acknowledges the financial support from the Ministry of Research, Technology, and Higher Education of the Republic of Indonesia for a scholarship through Riset-Pro (Loan number 8245-ID). A.A.F. wishes to acknowledge the access to research facilities within the School of Chemical and Process Engineering and G.M.K.'s laboratory without which this research would not have been possible to execute.

Conflicts of Interest: The authors declare no conflict of interest.

References

1. Choudhury, A.; Chandra, H.; Arora, A. Application of solid oxide fuel cell technology for power generation—A review. *Renew. Sust. Energ. Rev.* **2013**, *20*, 430–442. [CrossRef]
2. Conceiocao, L.D.; Silva, A.M.; Ribeiro, N.F.P.; Souza, M.M.V.M. Combustion synthesis of (LSCF) porous materials for application as cathode in IT-SOFC. *Mater. Res. Bull.* **2011**, *46*, 308–314. [CrossRef]

3. Vargas, R.A.; Bonturim, E.; Andreoli, M.; Chiba, R.; Seo, E.S.M. Characterization of LSCF-based composite and LSCF as cathodes for intermediate temperature SOFCs. *Mater. Sci. Forum* **2012**, *727–728*, 657–662. [CrossRef]
4. Badwal, S.P.S.; Giddey, S.; Munnings, C.; Kulkarni, A. Review of Progress in High Temperature Solid Oxide Fuel Cells. *J. Aust. Ceram. Soc.* **2014**, *50*, 23–37.
5. Sun, Y.; He, S.; Saunders, M.; Chen, K.; Shao, Z.; Jiang, S.P. A comparative study of surface segregation and interface of $La_{0.6}Sr_{0.4}Co_{0.2}Fe_{0.8}O_{3-\delta}$ electrode on GDC and YSZ electrolytes of solid oxide fuel cells. *Int. J. Hydrog. Energy* **2021**, *46*, 2606–2616. [CrossRef]
6. Simner, S.P.; Anderson, M.D.; Engelhard, M.H.; Stevenson, J.W. Degradation mechanisms of La-Sr-Co-Fe-O3SOFC cathodes Electrochem. *Solid State Lett.* **2006**, *9*, A478–A481. [CrossRef]
7. Wang, Z.; Kale, G.M.; Ghadiri, M. Synthesis and characterization of $Ce_xGd_{1-x}O_{2-\delta}$ nanopowders employing an alginate mediated ion-exchange process. *Chem. Eng. J.* **2012**, *198–199*, 149–153. [CrossRef]
8. Sardar, S.; Kale, G.; Ghadiri, M.; Cespedas, O. Structural Study of Holmium Zirconate Nanoparticles obtained through Carbon Neutral Sol-gel Process. *Thermochim. Acta* **2019**, *676*, 120–129. [CrossRef]
9. Rahayu, S.; Forrester, J.S.; Kale, G.M.; Ghadiri, M. Promising solid electrolyte material for an IT-SOFC: Crystal structure of the cerium gadolinium holmium oxide $Ce_{0.8}Cd_{0.1}Ho_{0.1}O_{1.9}$ between 295 and 1023 K. *Acta Cryst. Sect. C* **2018**, *74*, 236–239. [CrossRef] [PubMed]
10. Kosanke, K.L.; Kosanke, B.J.; Sturman, B.T.; Winokur, R.M. *Encyclopedic Dictionary of Pyrotechnics*; Journal of Pyrotechnics: Whitewater, WI, USA, 2012.
11. Wang, Z.; Kale, G.M.; Ghadiri, M. Novel Ion-Exchange Process for the Preparation of Metal Oxide Nanopowders from Sodium Alginate. *J. Am. Ceram. Soc.* **2012**, *95*, 3124–3129. [CrossRef]
12. Sardar, S.; Kale, G.M.; Cespedes, O.; Ghadiri, M. Environmentally sustainable facile synthesis of nanocrystalline Holmium Hafnate ($Ho_2Hf_2O_7$): Promising new oxide-ion conducting solid electrolyte. *Springer Nat. Appl. Sci.* **2020**, *2*, 541–552. [CrossRef]
13. Kale, G.M.; Jacob, K.T. Phase relations and thermodynamic properties of compounds in the pseudobinary system BaO-Y_2O_3. *Solid State Ion.* **1989**, *43*, 247–252. [CrossRef]
14. Hardy, J.S.; Templeton, J.W.; Edwards, D.J.; Lu, Z.; Stevenson, J.W. 2012. Lattice Expansion of LSCF-6428 Cathodes Measured by In-Situ XRD during SOFC Operation. *J. Power Sources* **2012**, *198*, 76–82. [CrossRef]
15. Cheng, J.; Zhang, M.; Jiang, Y.; Zou, L.; Gong, Y.; Chi, B.; Pu, J.; Jian, L. Perovskite $La_{0.6}Sr_{0.4}Co_{0.2}Fe_{0.8}O_3$ as an effective electrocatalyst for non-aqueous lithium air batteries. *Electrochim. Acta* **2016**, *191*, 106–115. [CrossRef]
16. Kuhn, J.N.; Ozkan, U.S. Effect of Co Content upon the Bulk Structure of Sr- and Co-doped $LaFeO_3$. *Catal. Lett.* **2008**, *121*, 179–188. [CrossRef]
17. Partovi, K.; Geppert, B.; Liang, F.; Rüscher, C.H.; Caro, J. Effect of the B-Site Composition on the Oxygen Permeability and the CO_2 Stability of $Pr_{0.6}Sr_{0.4}Co_xFe_{1-x}O_{3-\delta}$ ($0.0 \leq x \leq 1.0$) Membranes. *Chem. Mater.* **2015**, *27*, 2911–2919. [CrossRef]